Barisal University Journal Part 1, 4(2):299-311 (2017) ISSN 2411-247X

FIRST-PRINCIPLES STUDY OF ELECTRONIC AND OPTICAL PROPERTIES OF LEAD FREE ORGANIC-INORGANIC TIN HALIDE PEROVSKITES FOR PHOTOVOLTAIC APPLICATIONS

Md. Matiur Rahman*

*Department of Physics, University of Barisal, Barisal 8200, Bangladesh

Abstract

Organometallic perovskites ABX_3 are promising candidates, which have been passionately investigated during the last few years. In this work, we have calculated the geometry optimization, band structure which reveals a well-defined band gap at Fermi level, optical properties and charge carrier mobility for tetragonal phase of non-toxic perovskite of tin halide, $CH_3NH_3SnCl_3$ and $CH_3NH_3SnI_3$ by applying Density Functional Theory (DFT) with the Generalized Gradient Approximation (GGA) correlation of Perdew-Berke-Erzndof (PBE). The result have been showed that $CH_3NH_3SnCl_3$ and $CH_3NH_3SnI_3$ have good optical absorption coefficient, which can be used as solar light harvesters.

Keywords: First principle study, Perovskites, Organic-Inorganic Tin Halide, Solar harvester

Introduction

In the last few years, considerable and promising research on hybrid halide perovskite materials shown their potential applications as solar light absorbers (Chung et al., 2012; Burschka et al., 2013 and Kojima et al., 2009), topological insulators (Baugher et al., 2012), and superconductors (Takahashi et al. 2011). Methyl-ammonium metal-halide, with similar structure of ABX_3 (A = organic molecules, B = metal, X = halide) existing in nature, has been revealed as one of a potential material available for next-generation solar cell fabrications (Lang et al., 2014; Umari et al., 2014). Their potential applications included halide perovskite based solar cells with high efficiency, which reached 22.1% in 2016 (Best Research-Cell Efficiencies, www.nrel.gov/ncpv/images/ efficiency_chart. jpg

*Corresponding author's E-mail:matiurphys@gmail.com

(accessed: April 2016). n.d.), 17.9% in 2014 (Pascual Serrano et al. 2016), up as compared to dye sensitized solar cells (DSSCs) which had an efficiency of 3.8% in 2009 (Kojima et al. 2009). In the $CH_3NH_3Pb\mathit{X}_3$ (X = Cl, Br, I) lead compounds, cations $CH_3NH_3^+$rotate freely at high temperature because the potential barriers are smaller than the thermal energy that is confirmed experimentally by the nuclear magnetic resonance and nuclear quadrupole resonance (Knop et al., 1990), that at room temperature in the $CH_3NH_3Pb\mathit{X}_3$ cations $CH_3NH_3^+$ experience rapid isotropic orientation. In case of tin (II) based halide $CH_3NH_3Sn\mathit{X}_3$ compounds, similar behavior is found (Onoda-Yamamuro et al., 1995) in isostructural compounds. Earlier studies on compounds $CH_3NH_3Sn\mathit{X}_3$ showed that, transport properties seem to change from metallicity to semi-conductivity along the series I→Br→Cl (Yamada et al., 1990; Chiarella et al., 2007).

First-principles calculations can provide the possibility of designing new functional structures, with desired physical properties. In this research work, our objective was to investigate the possible clean, low cost, efficient and sustainable solar cells materials replacing lead based perovskites. We use DFT of GGA to optimize the structure and investigate the band structure, density of state, optical and electrical properties.

Computational Details

In this work we have done all the calculations, i.e, single point energy, geometry optimization, band structure, using the Kohn-Sham DFT calculation (Rajagopal et al., 1973; Kohn and Sham, 1965). The calculations was carried out with the energy-cutoff of 240eV and k-point grid of 2×2×2, under Monkhorst Pack (Pack and Monkhorst, 1977) special integration scheme, with brillouin sampling of 7 points. For band structure calculation, the total energy SCF tolerance was placed to a value of 2×10^6 eV/atom, with the maximum force of 0.05eV/Å, displacement of 0.002Å and maximum stress of 0.1GPa. The interaction of the valence core was provided, with the norm-conserving pseudopotential (Lin et al., 1993; Rappe et al., 1990), under Martin-Troullier scheme (Troullier and Martins, 1991), other than ultrasoft (Pickard and Payne, 2000) scheme, in evaluation of optical material properties, where the electron orbitals of, $2s^2\ 2p^2$ for C atom, $2s^2\ 2p^3$ for N atom, $5s^2\ 5p^2$ for Sn atom and $5s^2\ 5p^5$ for I atom were chosen.

For band structure calculation, the separation space of 0.025 $Å^{-1}$ and 12 empty bands at k point separation were employed. Here, the description of the GGA of PBE (Perdew, Burke and Ernzerhof, 1996) were treated when applying the exchange-correlation method. The geometry structure optimization and electronic structure calculations of halide perovskites ABX_3 were accomplished by using the Cambridge Sequential Total Energy Package (CASTEP) (Clark et al., 2005).

Results and Discussions

Tin based halide perovskite structure ABX_3 (A = CH_3NH_3; B = Sn; X = Cl, I), which are respectively shown in Fig.1. The geometry structure belongs to the tetragonal space groups 4/mmm. Metal B is bonded to six X anions, and BX_6 octahedral are corner-connected to form a three-dimensional framework.

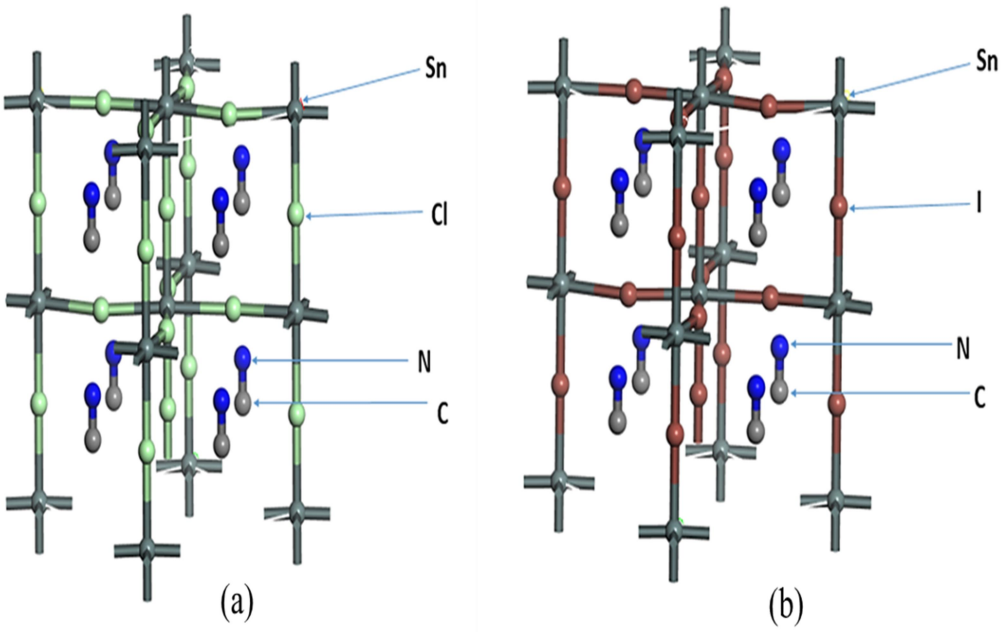

Fig. 1. Structure of $CH_3NH_3SnCl_3$ (a) and $CH_3NH_3SnI_3$ (b) perovskite.

The calculations of the electronic band structure help us to understand the character of prevailing bands near Fermi level, the energy in turns determine the properties of the material. The electronic band structures of $CH_3NH_3SnCl_3$ and $CH_3NH_3SnI_3$ are depicted in Fig. 2 (a) and (b) respectively. We find that $CH_3NH_3SnCl_3$ has a direct bandgap of 0.002 eV, shows semi-conducting properties and $CH_3NH_3SnI_3$ has overlapped bandgap that shows metallic character. We can also notice that the band gaps of $CH_3NH_3SnCl_3$ is larger than $CH_3NH_3SnI_3$. The reason for this is, the origin of valence band maximum (VBM) and conduction band minimum (CBM). The bandgap calculated by the PBE methods are not consistent with the experimental value because of not considering the spin orbit coupling (SOC).

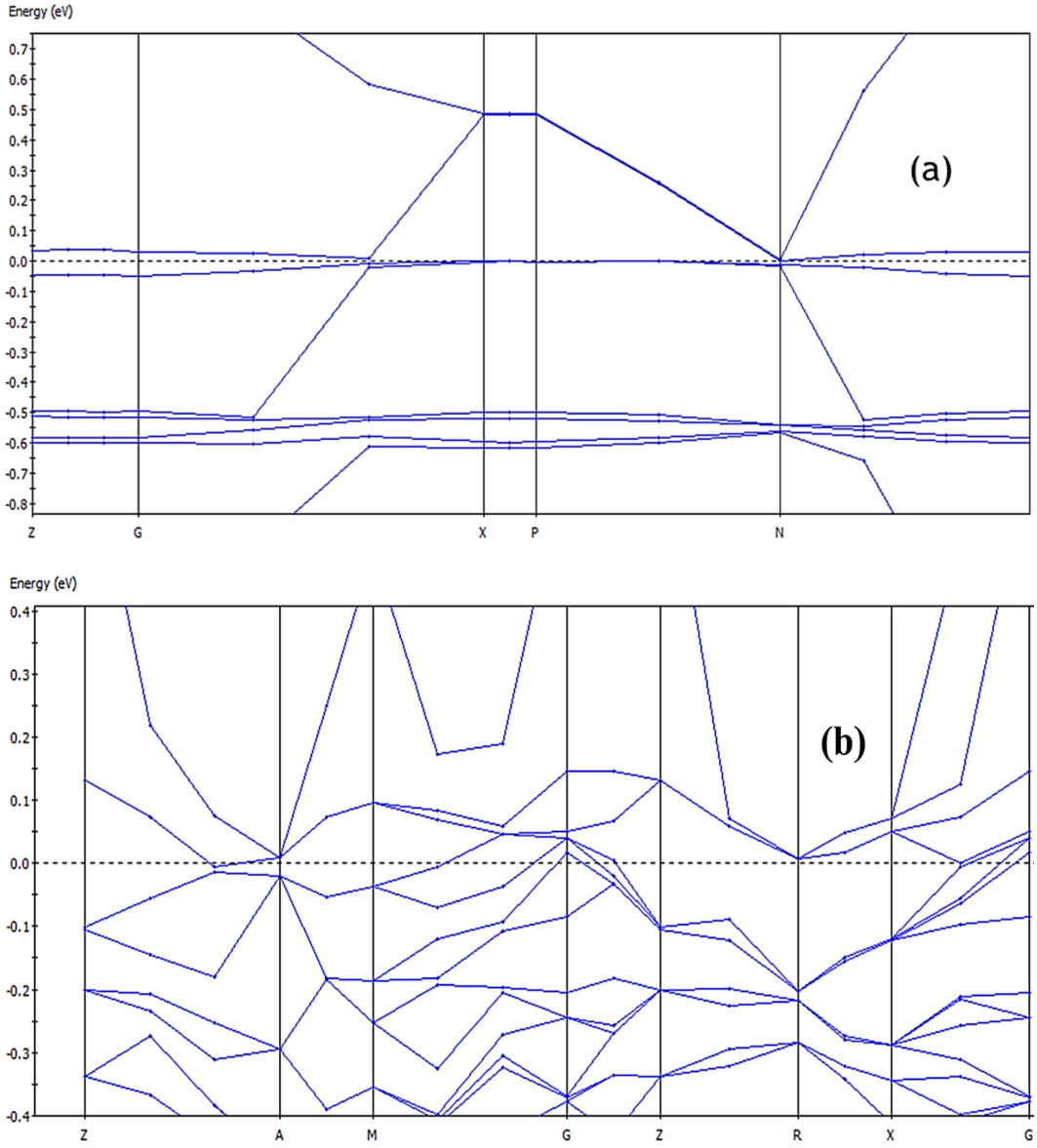

Fig. 2. (a) Band structure of $CH_3NH_3SnCl_3$ and (b) band structure of $CH_3NH_3SnI_3$ obtained using PBE method.

The lattice constants and band gaps of $CH_3NH_3BX_3$ found by using both PBE methods are recorded in Table 1. The obtained lattice constants of $CH_3NH_3SnI_3$ are in good agreement with experimental results as indicated in Table 1. The lattice constant of I is larger than Cl due to the larger atom I than that of Sn atom or Cl atom.

Table 1. Lattice constants and bandgap of ABX_3 using both PBE method.

ABX_3	Lattice Constants (Å)		Bandgap (eV)	
	PBE	*Experimental value*	*PBE*	*Experimental value*
$CH_3NH_3SnCl_3$	6.885 -	5.76 (Yamada et al., 1990) -	0.002	2.18 (Ananthajothi and Venkatachalam, 2015)
$CH_3NH_3SnI_3$	a = b = 8.594 c = 12.664	8.727 (Takahashi et al., 2011) 12.502 (Takahashi et al., 2011b)	0.0	1.30 (Yuan et al., 2015)

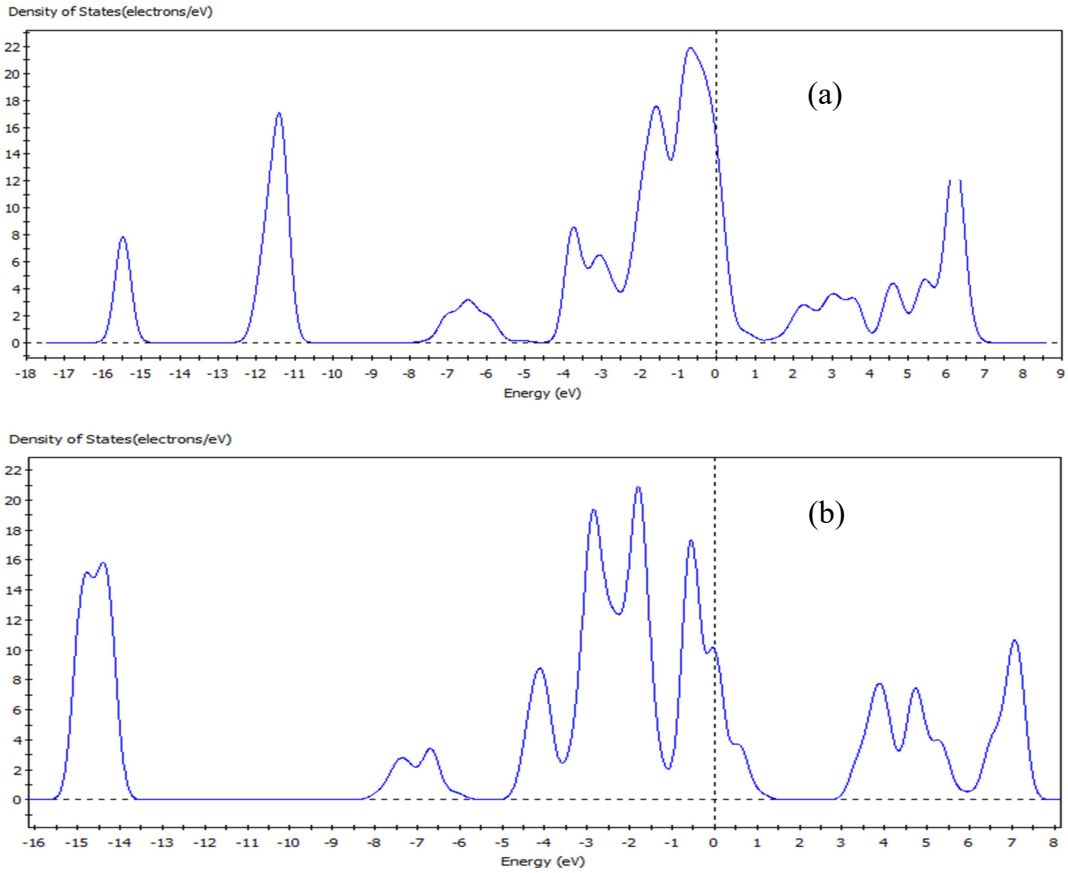

Fig. 3. Total DOS of (a) $CH_3NH_3SnCl_3$ and (b) $CH_3NH_3SnI_3$.

The density of states (DOS) of a system describes the number of states per interval of energy at each energy level that are available to be occupied. A DOS of zero means that no states can be occupied at that energy level. Fig. 3 shows the total density of states for $CH_3NH_3SnCl_3$ and $CH_3NH_3SnI_3$ calculated using PBE method. It is seen that the VBM and CBM of $CH_3NH_3SnCl_3$ is higher than $CH_3NH_3SnI_3$ for which the band gap of $CH_3NH_3SnCl_3$ is larger than $CH_3NH_3SnCl_3$.

Table 2. Bond distances between Sn-Cl and Sn-I of $CH_3NH_3SnCl_3$ and $CH_3NH_3SnI_3$ obtained by using PBE methods.

ABX_3	Bonds	Bond Length (Å)
$CH_3NH_3SnCl_3$	Cl 2 - Sn 2	1.189
	Cl 6 - Sn 2	2.677
$CH_3NH_3SnI_3$	I 2 - Sn 2	3.060
	I 6 - Sn 2	3.230

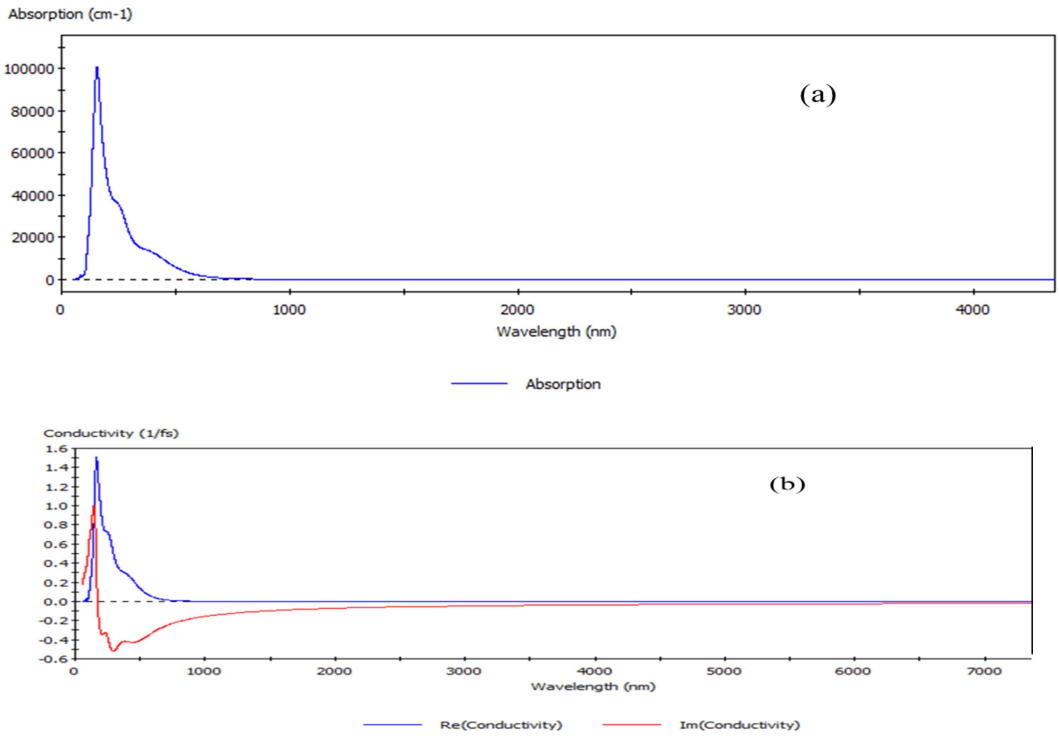

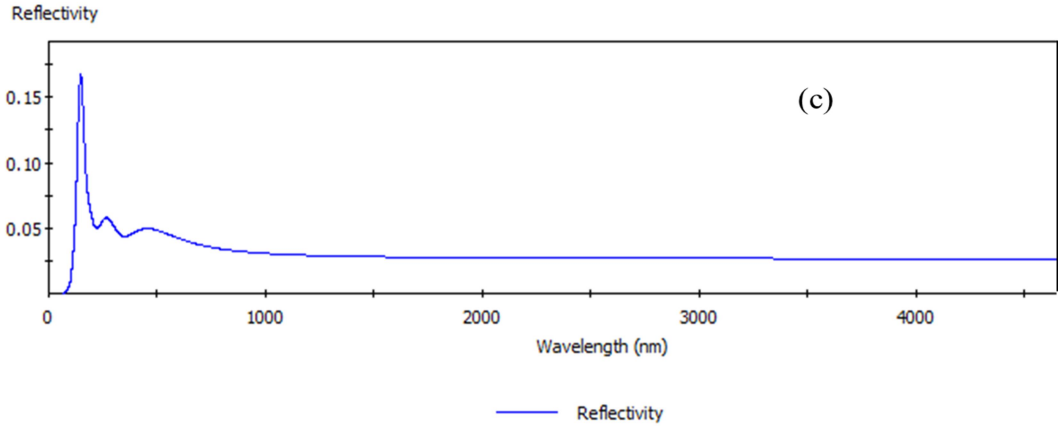
Reflectivity
0.15
0.10
0.05
(c)
0
1000
2000
3000
4000
Wavelength (nm)
Reflectivity

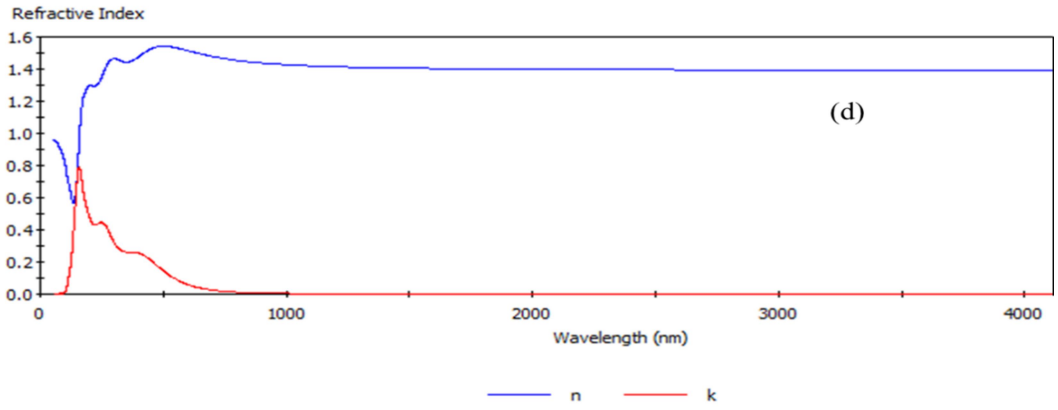
Refractive Index
1.6
1.4
1.2
1.0
0.8
0.6
0.4
0.2
0.0
(d)
0
1000
2000
3000
4000
Wavelength (nm)
n
k

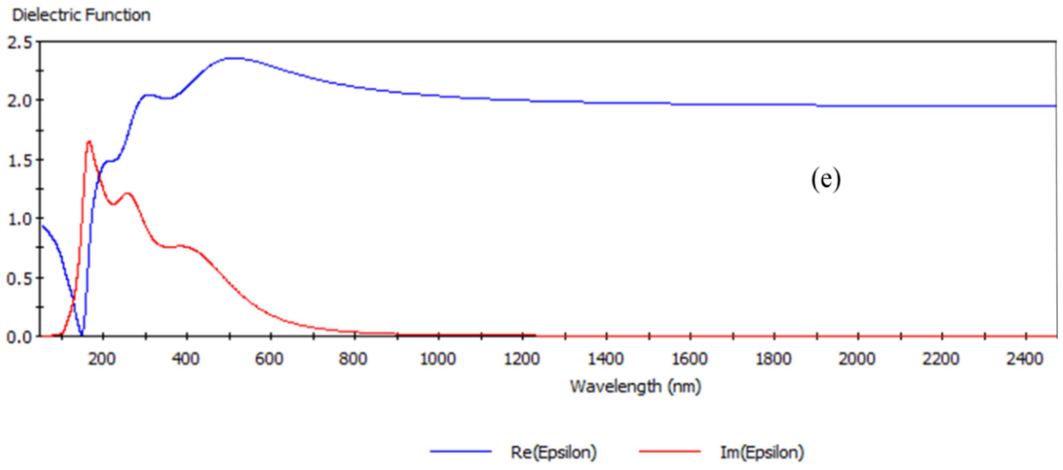
Dielectric Function
2.5
2.0
1.5
1.0
0.5
0.0
(e)
200
400
600
800
1000
1200
1400
1600
1800
2000
2200
2400
Wavelength (nm)
Re(Epsilon)
Im(Epsilon)

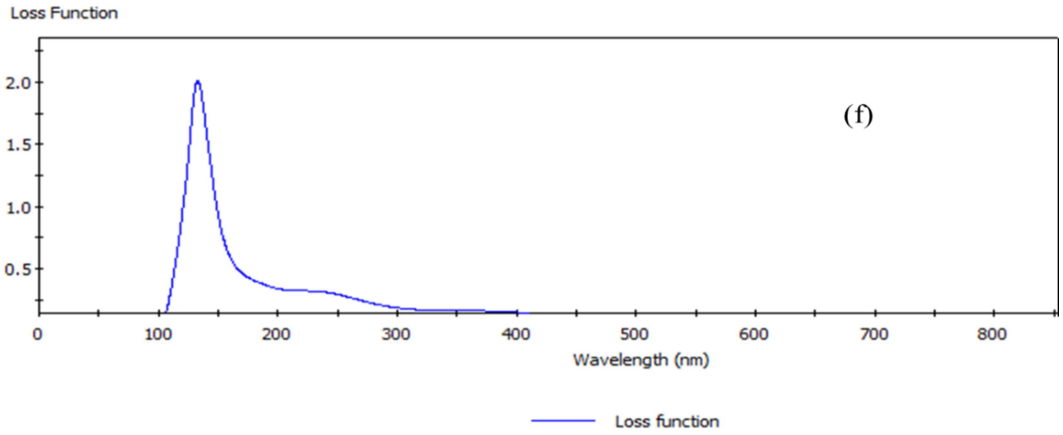

Fig. 4. (a), (b), (c), (d), (e) and (f) diagram illustrate the optical properties of $CH_3NH_3SnCl_3$.

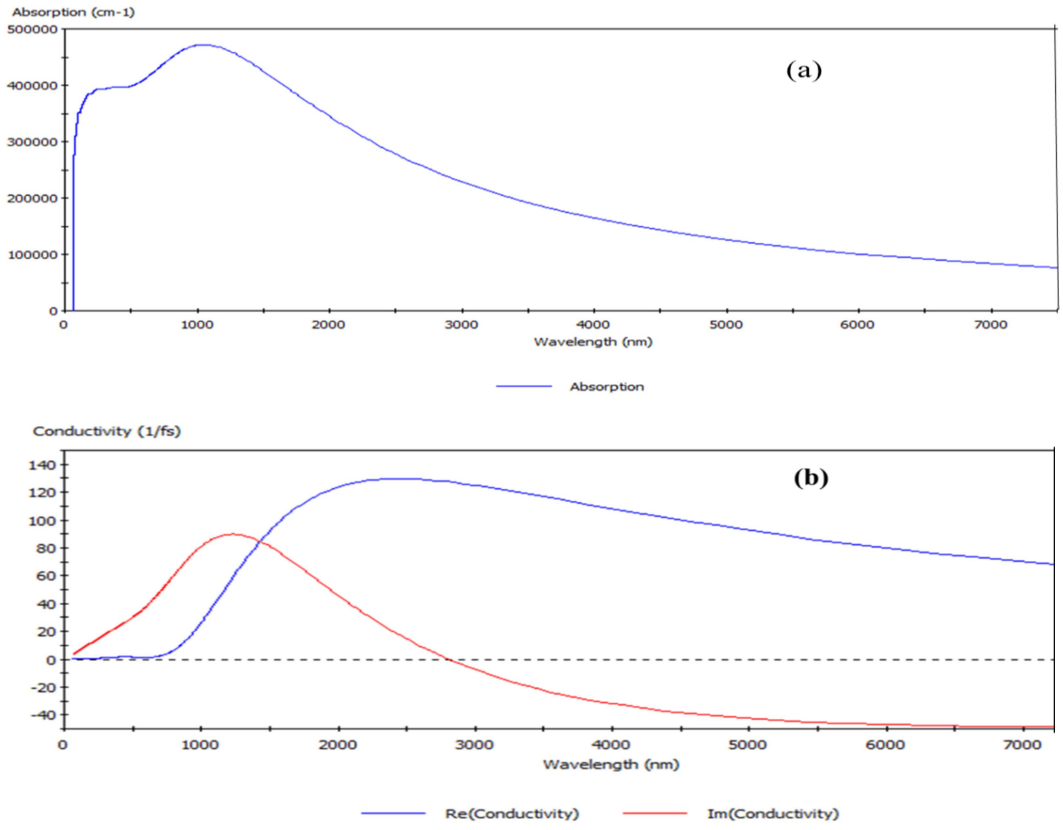

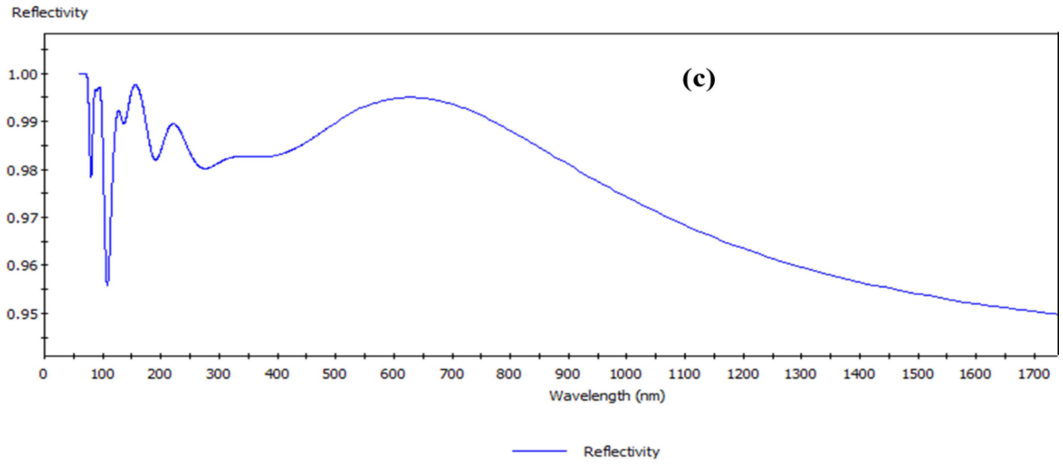
Reflectivity
(c)
1.00
0.99
0.98
0.97
0.96
0.95
0 100 200 300 400 500 600 700 800 900 1000 1100 1200 1300 1400 1500 1600 1700
Wavelength (nm)
Reflectivity

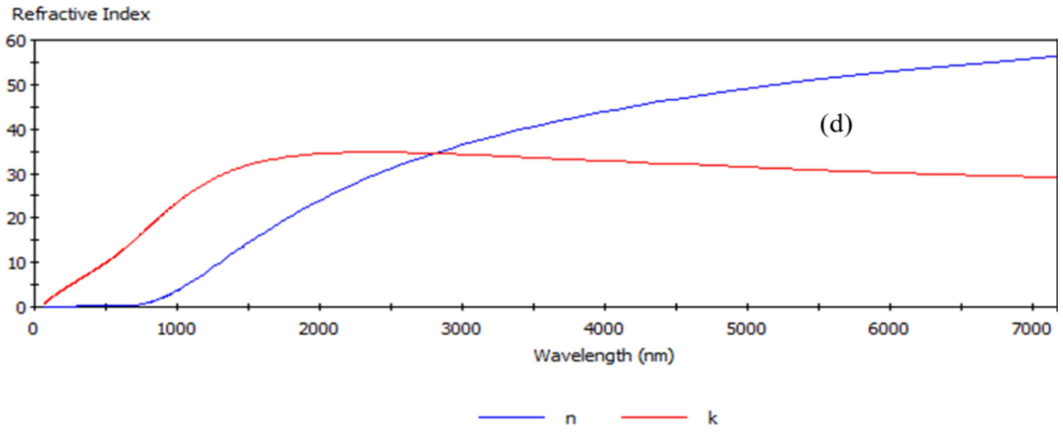
Refractive Index
(d)
60
50
40
30
20
10
0
0 1000 2000 3000 4000 5000 6000 7000
Wavelength (nm)
n
k

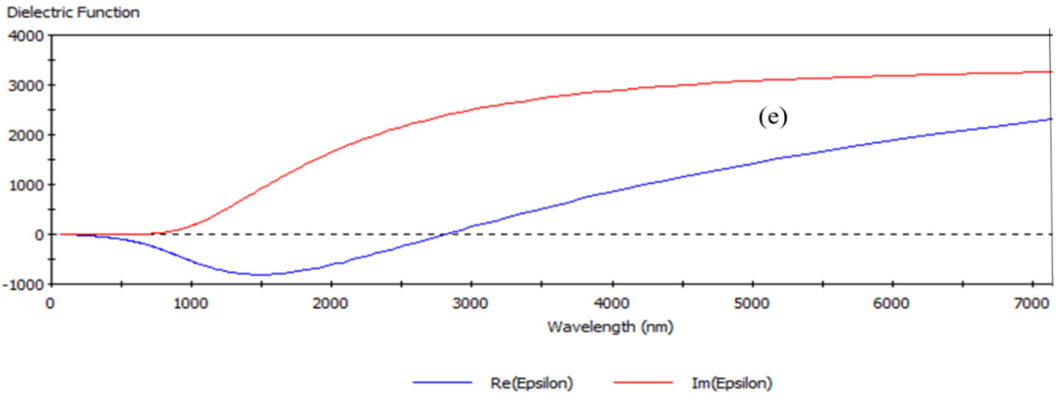
Dielectric Function
(e)
4000
3000
2000
1000
0
-1000
0 1000 2000 3000 4000 5000 6000 7000
Wavelength (nm)
Re(Epsilon)
Im(Epsilon)

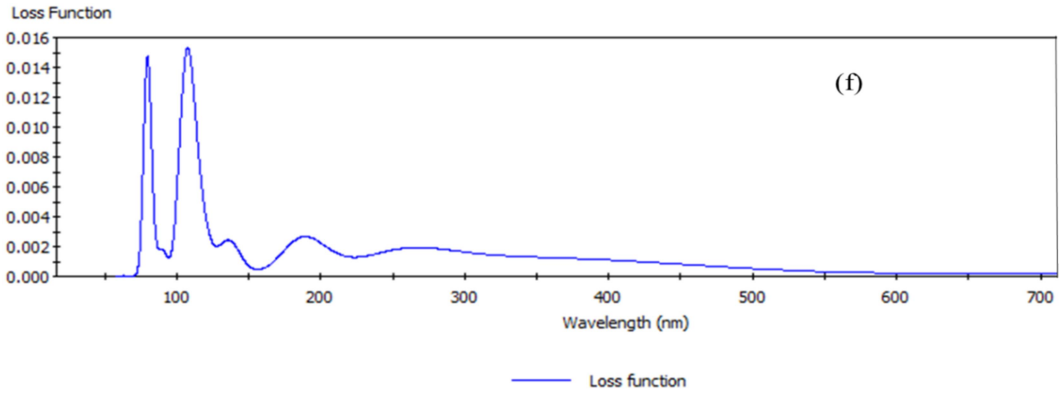

Fig. 5. (a), (b), (c), (d), (e) and (f) diagram illustrate the optical properties of $CH_3NH_3SnI_3$.

Optical properties are important in solid state physics for the study of the optical purposes of solids, deliver a better understanding of the electronic functions. From the figures, it is found that $CH_3NH_3SnCl_3$, the optical absorption was found indicating its peak ranges from 145 nm to 700 nm and have a peak at 320 nm near to the visible light spectrum. Therefore, $CH_3NH_3SnCl_3$ can harvest light in the visible region. For $CH_3NH_3SnI_3$, the absorption coefficient curve move away from violet to the red spectrum displaying red shift phenomenon and have a peak near to the visible light spectrum. It is clear that the $CH_3NH_3SnCl_3$ has higher absorption ability than that of $CH_3NH_3SnI_3$.

The optical conductivity of the $CH_3NH_3SnCl_3$ has a greater value than $CH_3NH_3SnI_3$ with respect to increasing wavelength as shown in Fig. 5 (b). The reflectivity of the each perovskite increase**s** with increasing wavelength but the percentage of reflection for both material is very low. The reflectivity spectrum shows that the materials are reflector within the wavelength range 150-950 nm for $CH_3NH_3SnI_3$, 120-200 nm for $CH_3NH_3SnCl_3$. In the energy-loss spectrums, the first peaks are found at 140nm for $CH_3NH_3SnCl_3$ and 110 nm for $CH_3NH_3SnI_3$. It indicates to a rapid reduction of the reflectance. Dielectric function is an important parameter for the study of optical properties and real part of it vanishes at about 7900 nm for each perovs kites. The refractive index of $CH_3NH_3SnCl_3$ is found to have the values 500 nm and of $CH_3NH_3SnI_3$ is 7500 nm. The above study suggest that, absorption of the $CH_3NH_3SnCl_3$ and $CH_3NH_3SnI_3$ is significantly intensive, which indicate that $CH_3NH_3SnCl_3$ and $CH_3NH_3SnI_3$ have superiority in utilizing solar energy.

Conclusions

The electronic structures of perovskites ABX_3 are studied by DFT using PBE approximations. We compare our calculated PBE results to experimental records for the

bandgap and we found that $CH_3NH_3SnCl_3$ has a direct bandgap which is consistent with the experimental result but the value is very poor. On the other hand $CH_3NH_3SnI_3$ has overlapped bandgap but the experimental value is 1.30 eV. The calculation at this level of approximation were only considered as a first approximation and had limited value as a quantitative prediction. The optical absorption was found indicating its peak near to the visible light spectrum. From the study of absorption, conductivity, reflectivity, refractive index, dielectric function and loss function, it can be concluded that the perovskites be useful in converting the sun radiation to electrical, which indicates their potential use as photovoltaic light absorbers. The simulation performances can be improved considering others hybrid functional like Heyd–Scuseria–Ernzerhof (HSE), spin orbit coupling (SOC), GW many-body corrections.

References

Akihiro Kojima T. M., K. Teshima and Y. Shirai. 2009. Organometal Halide Perovskites as Visible- Light Sensitizers for Photovoltaic Cells. Journal of American Chemical Society.**131:**6050-6051.

Ananthajothi and Venkatachalam. 2015. Synthesis and Optical Characterization of Cds, Cdse Quantum Dots and Ch3nh3sncl3 Perovskite Sensitizers Used in Solar Cell Applications. International Journal of Recent Scientific Research. **6:**6640-6644.

Baugher T., A. Gade, R. Janssens, S. Lenzi, D. Bazin, B. Brown, M. Carpenter, A. Deacon, S. Freeman, T. Glasmacher, G. Grinyer, F. Kondev, S. McDaniel, A. Poves, A. Ratkiewicz, E. McCutchan, D. Sharp, I. Stefanescu, K. Walsh, D. Weisshaar, and S. Zhu. 2012. Intermediate-energy Coulomb excitation of 58,60,62Cr: The onset of collectivity toward N = 40. Physical Review. *C.***86:**1-7.

Best Research-Cell Efficiencies, www.nrel.gov/ncpv/images/efficiency_chart. jpg (accessed: April 2016).

Burschka J., N. Pellet, S.-J. Moon, R. Humphry-Baker, P. Gao, M. K. Nazeeruddin, and M. Grätzel. 2013 Sequential deposition as a route to high-performance perovskite-sensitized solar cells. Nature. **499:**316-320.

Chiarella F., P. Ferro, F. Licci, M. Barra, M. Biasiucci, A. Cassinese, and R. Vaglio, 2006. Preparation and transport properties of hybrid organic–inorganic $CH_3NH_3SnBr_3$ films. Applied Physics A. **86:**89-93.

Chung I., B. Lee, J. He, R. P. H. Chang, and M. G. Kanatzidis. 2012. All-solid-state dye-sensitized solar cells with high efficiency. Nature. **485:**486-489.

Hohenberg, W., P.; Kohn. 1964. Inhomogeneous Electron Gas. Physical Review. **136:**B864-B871.

http://www.nrel.gov/ncpv/images/efficiency_chart.jpg.

Kim H.-S., C.-R. Lee, J.-H. Im, K.-B. Lee, T. Moehl, A. Marchioro, M. G. S.-J. Moon, R. Humphry-Baker, J.-H. Yum, J. E. Moserand N.-G. Park. 2012. Lead iodide perovskite sensitized all-solid-state submicron thin film mesoscopic solar cell with efficiency exceeding 9%. Scientific Reports. **2:**591-599.

Kohn W., and L. J. Sham. 1965. Self-consistent equations including exchange and correlation effects. Physical Review. **140:**A1134-A1138.

Lang L., J.-H. Yang, H.-R. Liu, H. J. Xiang, and X. G. Gong. 2014. First-principles study on the electronic and optical properties of cubic ABX_3 halide perovskites. Physics Letter A. **378:**290-293.

Lin, J. S., A. Qteish, M. C. Payne, and V. Heine. 1993. Optimized and transferable nonlocal separable ab initio pseudopotentials. Physical Review B. **47:**417-4180.

Monkhorst, H. J. and J. D. Pack. 1976. Special points for Brillouin-zone integrations. Physical Review B. **13:**5188-5192.

Onoda-Yamamuro, N., O. Yamamuro, T. Matsuo, H. Suga, K. Oikawa, N. Tsuchiya, T. Kamiyama, and H. Asano. 1995. Neutron-diffraction study of $CD_3ND_3SnBr_3$: Semiconductor-insulator transition with orientational ordering. Physica B: Physics of Condensed Matter. **213:**411-413.

Perdew J. P., K. Burke, and M. Ernzerhof. 1996. Generalized Gradient Approximation Made Simple. Physical Review Letter. **77:**3865-3868.

Pickard C. J., and M. C. Payne. 2000. Second-order k· p perturbation theory with Vanderbilt pseudopotentials and plane waves. Physical Review B. **62:**4383-4388.

Rappe A. M., K. M. Rabe, E. Kaxiras, and J. D. Joannopoulos, 1990. Optimized pseudopotentials. Physical Review B. **41:**1227-1230.

Takahashi Y., R. Obara, Z. Lin, Y. Takahashi, T. Naito, T. Inabe, S. Ishibashi and K. Terakura. 2011. Charge transport in tin-iodide perovskite: Origin of High Conductivity. Dalton Transactions. **40:**5563-5568.

Takahashi Y., R. Obara, Z.-Z. Lin, Y. Takahashi, T. Naito, T. Inabe, S. Ishibashi, and K. Terakura. 2011. Charge-transport in tin-iodide perovskite $CH_3NH_3SnI_3$: origin of high conductivity. Dalton Transactions. **40:**5563-5568.

Troullier N., and J. L. Martins. 1991. Efficient pseudopotentials for plane-wave calculations. II. Operators for fast iterative diagonalization. Physical Review B. **43:**886-8869.

Umari P., E. Mosconi, and F. De Angelis. 2014. Relativistic GW calculations on $CH_3NH_3PbI_3$ and CH3NH3SnI3 perovskites for solar cell applications. Scientific Reports. **4:**1-7.

Yamada KO. T., and I. S., Kawaguchi H, Matsui T. 1990. Structural Phase Transition and Electrical Conductivity of the Perovskite $CH_3NH_3Sn_{1-x}Pb_xBr_3$ and $CsSnBr_3$. Chemical Society of Japan. **63:**2521-2525.

Yamada, K., H. Kawaguchi, T. Matsui, T. Okuda, and S. Ichiba. 1990. Structural Phase Transition and Electrical Conductivity of the Perovskite $CH_3NH_3Sn_{1-x}PbxBr_3$ and CsSnBr3. Bulletin of the Chemical Society of Japan. **63:**2521-2525.

Yuan Y., R. Xu, H.-T. Xu, F. Hong, F. Xu, and L.-J. Wang. 2015. Nature of the band gap of halide perovskites ABX_3 (A = CH_3NH_3, Cs; B = Sn, Pb; X = Cl, Br, I): First-principles calculations. Chinese Physics. B. **24:**1-5.